miR-187-3p inhibitor attenuates cerebral ischemia/reperfusion injury by regulating Seipin-mediated autophagic flux

ZHENKUI REN[1-3], PENG XIE[1,2], JU LV[1,2], YUMEI HU[1,2], ZHIZHONG GUAN[1,2,4], LING CHEN[5] and WENFENG YU[1,2]

[1]Key Laboratory of Endemic and Ethnic Diseases, Ministry of Education, School of Basic Medical Science, Guizhou Medical University; [2]Key Laboratory of Medical Molecular Biology, Guizhou Medical University, Guiyang, Guizhou 550004; [3]Laboratory Department of People's Hospital of Southwest Guizhou Autonomous Prefecture, Xingyi, Guizhou 562400; [4]Department of Pathology, Affiliated Hospital of Guizhou Medical University, Guiyang, Guizhou 550004; [5]Laboratory of Reproductive Medicine, Department of Physiology, Nanjing Medical University, Nanjing, Jiangsu 210029, P.R. China

Received January 21, 2020; Accepted May 22, 2020

DOI: 10.3892/ijmm.2020.4642

Abstract. MicroRNAs (miRNAs/miRs) have been reported to affect ischemia/reperfusion (I/R)-induced cerebral damage. miRNAs cause post-transcriptional gene silencing by binding to the protein-coding sequence (CDS) of mRNAs. Seipin has a potential role in regulating autophagic flux. The present study investigated the involvement of miR-187-3p in Seipin expression, autophagic flux and apoptosis *in vitro*, as well as the underlying mechanism, using PC12 cells exposed to oxygen-glucose deprivation/reoxygenation (OGD/R), which mimicked the process of I/R. In comparison with control PC12 cells, OGD/R caused an increase in the level of miR-187-3p and a decrease in Seipin protein levels without changes in the level of Seipin mRNA. Using bioinformatics analysis, it was identified that miR-187-3p could bind to the CDS of Seipin. miR-187-3p inhibitor attenuated the reduction in Seipin protein expression in OGD/R-treated PC12 cells. Following OGD/R, autophagic flux was reduced and apoptosis was enhanced, which were attenuated by inhibition of miR-187-3p. Compared with OGD/R-treated PC12 cells, Seipin knockdown further impaired autophagic flux and promoted neuronal apoptosis, which were insensitive to inhibition of miR-187-3p. Furthermore, treatment with miR-187-3p inhibitor could decrease the infarction volume in a rat model of middle cerebral artery occlusion/reperfusion. The present findings indicated that miR-187-3p inhibitor attenuated ischemia-induced cerebral damage by rescuing Seipin expression to improve autophagic flux.

Correspondence to: Professor Ling Chen, Laboratory of Reproductive Medicine, Department of Physiology, Nanjing Medical University, 140 Hanzhong Road, Nanjing, Jiangsu 210029, P.R. China
E-mail: lingchen@njmu.edu.cn

Professor Wenfeng Yu, Key Laboratory of Endemic and Ethnic Diseases, Ministry of Education, School of Basic Medical Science, Guizhou Medical University, 9 Beijing Road, Guiyang, Guizhou 550004, P.R. China
E-mail: wenfengyu2013@126.com

Key words: microRNA-187-3p, Seipin, autophagic flux, apoptosis, ischemia/reperfusion

Introduction

Cerebral ischemia/reperfusion (I/R)-related disability, which is characterized by inflammation, necrosis and apoptosis of cells, represents a significant healthcare burden worldwide, causing 6.5 million deaths every year (1-3). Autophagy plays important roles in the pathology of cerebral I/R (4). Numerous neuroprotective agents have been shown to be effective in animal experiments; however, they were reported to be ineffective in clinical trials (5-7). Thus, a deeper exploration of the molecular mechanisms underlying cerebral I/R injury and the identification of novel therapeutic targets to control cerebral I/R-associated brain injury is urgently required.

During the last decade, substantial efforts have been undertaken to isolate and identify microRNAs (miRNAs/miRs), and investigate their functions *in vitro* and *in vivo* (8-10). As functional RNA molecules that can inhibit protein expression by targeting the 3'-untranslated region (3'-UTR) of target mRNAs, miRNAs are involved in numerous physiological and pathological processes (11). Cerebral miRNA profiles are reportedly significantly altered and affect disease outcomes in central nervous system (CNS) diseases, which has led to an explosion of potential biomarkers for these diseases (12,13). miRNAs associated with the regulation of apoptosis and autophagy during ischemic stroke have been identified (14,15). miRNA binding sites in the coding sequences (CDSs) of mRNAs have been predicted by combining computational approaches and human mRNA expression data (16). Numerous studies have provided experimental evidence of the existence of functional miRNA binding sites in mammalian CDSs (17-20).

For example, miR-148 inhibits DNA methyltransferase 3β expression by targeting a conserved site in its CDS (17).

Seipin is an endoplasmic reticulum membrane protein that is encoded by the Berardinelli-Seip congenital lipodystrophy type 2 (*BSCL2/Bscl2*) gene (21-23). Seipin is a widely expressed protein but with highest levels found in the CNS of humans (24). Using immunohistochemistry, Seipin expression has been detected in neurons of the frontal lobe cortex of the brain, including the motor and somatosensory cortex (25). Recently, the transcript encoding the long Seipin isoform (BSCL2-203, 462 amino acids) was reported to be expressed primarily in the brain, and its expression was inversely correlated with age in neuronal cells (24). Seipin deficiency has been reported to aggravate I/R-induced cerebral damage (26). Seipin mutations at glycosylation sites result in the activation of autophagy (27,28). Our recent study reported that neuronal Seipin deletion reduces autophagosome formation to cause hyperphosphorylation and aggregation of tau protein through reduced inhibition of peroxisome proliferator-activated receptor γ in Akt/mTOR signaling (29). Furthermore, miRNAs have been associated with autophagy and apoptosis in brains following ischemic stroke (30,31). Therefore, if cerebral ischemia alters miRNA and Seipin levels, it is of great interest to investigate whether alterations in miRNA expression affect the expression of Seipin, and autophagy and apoptosis.

The present study evaluated the involvement of miR-187-3p in Seipin expression, autophagic flux and apoptosis after ischemic stroke, or in PC12 cells treated with oxygen-glucose deprivation and reoxygenation (OGD/R), and explored the underlying molecular mechanisms. The results of the present study indicated that the OGD/R-induced increase in the levels of miR-187-3p suppressed Seipin expression, leading to a deficit in autophagic flux and neuronal apoptosis.

Materials and methods

Cells, culture and OGD/R model establishment. PC12 cells and 293T cells were purchased from the Cell Bank of Shanghai Institute of Cell Biology. PC12 cells and 293T cells were incubated in Dulbecco's modified Eagle's medium (DMEM; Invitrogen; Thermo Fisher Scientific, Inc.) containing 10% fetal bovine serum, 100 μg/ml streptomycin and 100 U/ml penicillin (all from Gibco; Thermo Fisher Scientific, Inc.) at 37˚C with 5% CO_2. For OGD/R treatment, PC12 cells were incubated in glucose-free DMEM (Invitrogen; Thermo Fisher Scientific, Inc.) and incubated at 37˚C in the presence of 5% CO_2 and 95% N_2 for 4 h, followed by 18 h of reoxygenation.

Identification of miRNAs targeting Seipin. Total RNA, including miRNA, was extracted using TRIzol® reagent (Invitrogen; Thermo Fisher Scientific, Inc.) from control and 4:18-h OGD/R-exposed PC12 cells. High-throughput next-generation sequencing was used for miRNA sequencing to achieve optimal PC12 cell miRNA profiles. miRNA sequencing was carried out using a high-throughput Illumina HiSeq 2000 sequencing platform (BGI Group). miRNAs with a Q-value ≤0.01 and |log (fold-change)|>2 were considered differentially expressed. miRNAs targeting the CDS of Seipin were predicted using the miRanda database (http://www.microrna.org/microrna/home.do).

Seipin short hairpin (sh)RNA design and lentivirus construction. Seipin expression was knocked down in PC12 cells using a targeted shRNA. Short hairpin RNA (shRNA) specific for Seipin (5'-ACGCTCGGTGATGCTTCATTA-3') and a non-targeting scramble shRNA sequence (5'-TTCTCC GAACGTGTCACGT-3') construct were designed and cloned into a hU6-MCS-Ubiquitin-EGFP-IRES-puromycin vector, and packaged into a lentivirus (Shanghai GeneChem Co., Ltd.). The lentiviral constructs (MOI=70) were infected into PC12 cells ($5x10^5$ cells/cm^2) for the generation of stable clones according to the manufacturer's instructions. At 48 h after transduction, PC12 cells were treated with 4:18-h OGD/R. For experiments involving rapamycin (Sigma-Aldrich; Merck KGaA) treatment, rapamycin (20 nM) was added to the culture medium 2 h before PC12 cells were subjected to OGD/R.

Cell transfection. miR-187-3p mimics (sense, 5'-UCGUGU CUUGUGUUGCAGCCGG-3'; antisense, 5'-CCGGCUGCA ACACAAGACACGA-3'), miR-187-3p inhibitor (5'-CCGGCU GCAACACAAGACACGA-3'), mimics negative control (NC; sense, 5'-UUUGUACUACACAAAAGUACUG-3'; antisense, 5'-CAGUACUUUUGUGUAGUACAAA-3') and inhibitor NC (5'-CAGUACUUUUGUGUAGUACAAA-3') were purchased from Guangzhou RiboBio Co., Ltd. and transfected into PC12 cells ($5x10^5$ cells/cm^2) using riboFECT™ CP transfection reagent (Guangzhou RiboBio Co., Ltd.) according to the manufacturer's instructions (50 nM). Cells were collected for further experiments after 48 h of transfection.

Adenovirus (Ad)-mRFP-GFP-LC3 transfection and confocal microscopy. PC12 cells were cultured in 24-well plates at a density of $1x10^4$ cells/well and transfected with miR-187-3p mimics, inhibitor or mimics NC. After 12 h, cells were infected with an Ad-mRFP-GFP-LC3 vector (Hanbio Biotechnology Co., Ltd.) at MOI=30 for a further 24 h. Then, PC12 cells were incubated in glucose-free DMEM (Invitrogen; Thermo Fisher Scientific, Inc.) and incubated at 37˚C in the presence of 5% CO_2 and 95% N_2 for 4 h, followed by 18 h of reoxygenation. Fluorescent puncta were detected in PC12 cells infected with Ad-mRFP-GFP-LC3 via Olympus laser scanning confocal microscopy (magnification, x100; Olympus Corporation). Yellow and red represent autophagolysosomes and autophagosomes, respectively; 20 cells/group were analyzed.

Reverse transcription-quantitative (RT-q)PCR. Total RNAs (including miRNAs) were extracted from PC12 cells or brain tissues using TRIzol reagent (Invitrogen; Thermo Fisher Scientific, Inc.) according to the manufacturer's protocol. miRNAs were transcribed into cDNA (25˚C for 5 min, 50˚C for 15 min and 85˚C for 5 min) using an miRNA 1st-Strand cDNA Synthesis kit (Vazyme Biotech Co., Ltd.). miR-187-3p expression was quantified by RT-qPCR using an miRNA Universal SYBR qPCR Master Mix kit (Vazyme Biotech Co., Ltd.), and U6 small nuclear RNA served as an internal reference for normalization. For mRNA expression analysis, cDNA was synthesized (42˚C for 15 min and 85˚C for 5 min) using StarScript II First-strand cDNA Synthesis Mix With gDNA Remover kit (GenStar). qPCR was performed using SYBR-Green SuperMix (Vazyme Biotech Co., Ltd.) as follows: At 95˚C for 3 min, followed by 39 cycles of 60˚C for 30 sec and 70˚C for 15 sec. The following primers were

used (Sangon Biotech Co., Ltd.): U6, forward, 5'-CTCGCTTCG GCAGCACA-3' and reverse, AACGCTTCACGAATTTGCGT; miR-187-3p, forward 5'-AGCGTCGTGTCTTGTGTTGC-3' and reverse, 5'-GTCGTATCCAGTGCAGGGTCCGAGGTATTC GCACTGGATACGACCCGGCT-3'; Seipin, forward, 5'-AGG TGGCCGAATCATCTCCA-3' and reverse, 5'-GAGAACACC AGCGTGTCGAG-3'; GAPDH, forward, 5'-AGGTCGGTG TGAACGGATTTG-3' and reverse, 5'-GGGGTCGTTGAT GGCAACA-3'. The relative expression levels of miRNAs and Seipin mRNA were calculated using the $2^{-\Delta\Delta Cq}$ method (32).

Luciferase reporter assay. Fragments of the wild-type Seipin CDS containing two miR-187-3p target sites, and mutants of these respective sites were amplified and cloned into a psiCHECK™-2 vector (Promega Corporation). 293T cells were seeded in 96-well plates 1 day before transfection. When the cell density reached ~50%, the cells were co-transfected with the psiCHECK-2 vector (0.16 μg) containing the CDS of Seipin [with wild-type (Seipin-wt), mutant miR-187-3p binding site 1 (Seipin-mu1) or mutant miR-187-3p binding site 2 (Seipin-mu2)], and miR-187-3p mimics (5 pmol) or mimics NC (5 pmol) with riboFECT CP. After transfection for 48 h, the cells were analyzed using a Dual-Luciferase Reporter Assay System (Promega Corporation) according to the manufacturer's protocols. Data were calculated as the ratio of *Renilla* to firefly luciferase activity.

Western blotting. Cells were seeded in a 6-well plate and washed three times with pre-cooled PBS. Then, 60 μl RIPA buffer (Thermo Fisher Scientific, Inc.) containing protease inhibitor cocktail (Sigma-Aldrich; Merck KGaA) was added to each well, and the plate was placed on ice for ~2 h; Total proteins were extracted from the rat cortical peri-infarct region using RIPA buffer (Thermo Fisher Scientific, Inc.) containing protease inhibitor cocktail (Sigma-Aldrich; Merck KGaA). Proteins were quantified using a bicinchoninic acid assay kit (cat. no. P0009; Beyotime Institute of Biotechnology). Proteins (25 μg) were separated by 12% SDS-PAGE and transferred onto nitrocellulose membranes. The membrane was blocked with 5% nonfat milk at room temperature for 2 h and then incubated with primary antibodies against the autophagy-related proteins phosphorylated (p)-mTOR (1:1,000; cat. no. 5536S; Cell Signaling Technology, Inc.), mTOR (1:1,000; cat. no. 2972S; Cell Signaling Technology, Inc.), p62 (1:1,000; cat. no. 23214; Cell Signaling Technology, Inc.) and light chain (LC)3II/I (1:1,000; cat. no. 4108S; Cell Signaling Technology, Inc.), the apoptosis-related proteins cleaved caspase-3 (1:1,000; cat. no. 9661S; Cell Signaling Technology, Inc.), Bax (1:1,000; cat. no. ab32503; Abcam), and Seipin (1:1,000; cat. no. ab106793; Abcam) and β-actin (1:1,000; cat. no. 3700S; Cell Signaling Technology, Inc.) at 4˚C overnight. Membranes were then incubated at room temperature for 2 h with the horseradish peroxidase-conjugated secondary antibody (1:1,000; cat. no. 7074S; Cell Signaling Technology, Inc.), and an enhanced chemiluminescence reagent kit (Amersham; Cytiva) was used for visualization. Gray values of autophagy- and apoptosis-related proteins were measured using ImageJ software (version 1.42q, National Institutes of Health) and normalized to that of β-actin as an internal control.

Detection of apoptosis by flow cytometry. Seipen shRNA-expressing PC12 cells were seeded in a 6-well plate at $1x10^6$ cells/well and exposed to miR-187-3p inhibitor or inhibitor NC (50 nM) for 48 h. Then, normoxic control and OGD/R PC12 cells were prepared as described above. After three washes with pre-cooled PBS, 100 μl of the cell suspension was collected. The cells were stained with 5 μl of Annexin V-allophycocyanin and 10 μl of 7-aminoactinomyosin D (MultiSciences Biotech Co., Ltd.) at 37˚C for 10 min in the dark. Binding buffer (400 μl) was subsequently added to each sample, and apoptosis was detected by flow cytometry (BD Accuri C6 Flow Cytometer; BD Biosciences). Flow cytometric data were analyzed using FlowJo version 8.6 (FlowJo LLC). The apoptosis rate was calculated as the percentage of early + late apoptotic cells.

Rat model of focal cerebral I/R. The present study was approved by the Animal Care and Use Committee of Guizhou Medical University (permit no. 1900813). A total of 54 male Sprague-Dawley rats (2 months old; weight, 250-300 g) were obtained from the Experimental Animals Center at Guizhou Medical University. Rats were housed under comfortable conditions (12:12-h light/dark cycle, humidity 55-60%, 20-25˚C, and access to food and water *ad libitum*). 18 rats were used in each group (6 rats for infarct size measurement, 6 rats for expression analysis, 6 rats for immunofluorescence). Reperfusion was established 1 h after middle cerebral artery occlusion (MCAO) as previously reported (33). The animals were anesthetized with chloral hydrate 10% (300 mg/kg) and the rectal temperature was maintained at 37.0±0.5˚C throughout the operation. No rats exhibited signs of peritonitis after administration of 10% chloral hydrate. At 24 h after reperfusion, the rats were sacrificed, and their brains were collected. Sham rats underwent the same surgical procedure, except without MCAO. Rat euthanasia was conducted via CO_2 inhalation; rats were placed into enclosed flow cages for 5 min, and 100% CO_2 was then added to the cages at a displacement rate of 30% volume/min (34). After euthanasia, death was confirmed via decapitation and brains were collected.

Intracerebroventricular injection. miR-187-3p antagomir and antagomir NC (1.5 nmol/200 g), synthesized by Guangzhou RiboBio Co., Ltd. (same sequences as miR-187-3p inhibitor and inhibitor NC, respectively), were dissolved in 0.9% saline (1.5 nmol/6 μl saline) and administered to rats 2 h before MCAO though intraventricular injection as previously described (35). Rats were anesthetized and placed on a stereotactic head frame (RWD Life Science). miR-187-3p antagomir and antagomir NC were infused slowly into the right lateral ventricle using a micro-infusion pump (KDS 310; KD Scientific) at a rate of 0.2 μl/min. To prevent possible leakage, the burr hole was sealed with bone wax. The incision was sutured and rats were placed into cages for recovery, then rats were given free access to food and water.

Determination of infarct size. According to a previously described method (33), after 24 h reperfusion, the brains were collected and stored at -20˚C for 20 min before sectioning sectioned coronally at a thickness of 1 mm. Briefly, the sections were stained with tetrazolium chloride (0.2%) at 37˚C for 30 min and imaged with a digital camera. The infarct volume

was corrected for possible interference from brain edema and presented as a ratio of the infarct volume compared with the contralateral hemisphere volume.

Immunofluorescence assay. Rats were perfused transcardially with 4% paraformaldehyde. The frozen brains were mounted on a freezing (-80˚C) microtome and cut into 30-μm sections (Leica Microsystems GmbH). Frozen sections (n=4/rat) were blocked and permeabilized with 5% normal goat serum (Sigma-Aldrich; Merck KGaA) and 0.3% Triton X-100 for 1 h at room temperature. The slices were then incubated overnight at 4˚C with a primary antibody against LC3 (1:200; cat. no. 4108S; Cell Signaling Technology, Inc.) followed by incubation with Alexa Fluor® 568-conjugated goat anti-rabbit IgG (H + L) cross-adsorbed secondary antibody (1:100; cat. no. A-11011; Thermo Fisher Scientific, Inc.) for 1 h at room temperature. After washing, nuclei were counterstained with DAPI (Beyotime Institute of Biotechnology) for 5 min at room temperature. Images were collected with a Laser confocal microscope (magnification, x20; Olympus FV 1000; Olympus Corporation); 20 fields/section were randomly analyzed.

Statistical analysis. Statistical analysis was conducted using GraphPad Prism software 7.0 (GraphPad Software, Inc.). Data are presented as the mean ± SD. Comparisons among multiple groups were performed using one-way ANOVA followed by Tukey's post hoc test; unpaired t-tests were used for comparisons between two groups. P<0.05 was considered to indicate a statistically significant difference.

Results

miR-187-3p is upregulated and Seipin protein is downregulated in OGD/R PC12 cells. RNA-seq analysis in 4:18-h OGD/R-treated PC12 cells revealed that 89 miRNAs were upregulated and 66 miRNAs were downregulated (Fig. 1A). Using bioinformatics analysis, 76 miRNAs targeting the CDS of Seipin were identified (Fig. 1B). A heatmap revealed that 18 miRNAs were significantly differentially expressed with a fold change >1, including miR-187-3p (Fig. 1C). RT-qPCR analysis showed that miR-187-3p levels were increased in OGD/R PC12 cells compared with control cells (n=3; P<0.05; Fig. 1D), whereas the level of Seipin mRNA was unchanged (n=3; P>0.05; Fig. 1E). However, the results from western blotting found that the levels of Seipin protein were significantly decreased in OGD/R PC12 cells (n=3; P<0.05; Fig. 1F). The results indicated that the increased miR-187-3p may directly alter the Seipin expression.

Seipin is a downstream target of miR-187-3p. To test whether miR-187-3p reduced Seipin expression in OGD/R PC12 cells, two miR-187-3p binding sites were predicted in the CDS of Seipin using miRanda (Fig. 2A). As shown in Fig. 2B, a luciferase assay validated Seipin as a target of miR-187-3p, indicating that miR-187-3p can regulate Seipin expression and function. Co-transfection of a dual-luciferase reporter plasmid containing the Seipin-wt or Seipin-mu1 CDS of Seipin and miR-187-3p mimics caused a decrease in the reporter activity (P<0.01; Fig. 2B); only the Seipin-mu2 mutant effectively produced reporter activity. Fig. S1A demonstrated that miR-187-3p mimic increased the expression of miR-187-3p compared with mimic NC in the absence of any other treatment, whereas miR-187-3p inhibitor decreased the expression of miR-187-3p compared with inhibitor NC group in the absence of any other treatment (Fig. S1B). Neither overexpression of miR-187-3p by mimics nor inhibition of miR-187-3p by inhibitor in PC12 cells altered the levels of Seipin mRNA (n=3; P>0.05; Fig. 2C). However, the administration of miR-187-3p mimics in PC12 cells reduced the levels of Seipin protein (n=3; P<0.05; Fig. 2D), whereas miR-187-3p inhibitor partially reversed the reduction in Seipin protein expression in OGD/R PC12 cells (n=3; P<0.01; Fig. 2E). The results indicated that the increase in miR-187-3p suppressed Seipin expression in OGD/R PC12 cells.

Increased miR-187-3p disturbs autophagic flux and aggravates apoptosis in OGD/R PC12 cells. To test whether miR-187-3p is involved in alterations in autophagic flux and apoptosis, OGD/R-treated PC12 cells were transfected with miR-187-3p mimics or inhibitor. It was determined by qPCR that miR-187-3p mimics caused a significant increase in the levels of miR-187-3p in OGD/R PC12 cells compared with mimics NC-transfected OGD/R-treated PC12 cells (n=3; P<0.05), whereas miR-187-3p inhibitor reduced miR-187-3p levels in OGD/R PC12 cells (n=3; P<0.05; Fig. 3A). In comparison with mimics NC-transfected OGD/R PC12 cells, exogenously overexpressing miR-187-3p in OGD/R-treated PC12 cells aggravated the impairment of autophagic flux and increased apoptosis; the levels of p62 were higher (n=3; P<0.05; Fig. 3C and D) and the LC3II/I ratio was lower (n=3; P<0.05; Fig. 3C and E), but also the levels of cleaved caspase-3 (n=3; P<0.05; Fig. 3C and F) and Bax (n=3; P<0.05; Fig. 3C and G) were higher. By contrast, the miR-187-3p inhibitor in OGD/R PC12 cells decreased the levels of p62 (n=3; P<0.05), increased the LC3II/I ratio (n=3; P<0.05), and decreased the levels of cleaved caspase-3 (n=3; P<0.05) and Bax (n=3; P<0.05), indicating that autophagic flux was recovered and apoptosis was decreased. The results indicated that increased miR-187-3p causes impairment of autophagic flux and apoptosis in OGD/R-treated PC12 cells.

Reduced Seipin disturbs autophagic flux and aggravates apoptosis in OGD/R PC12 cells. These results indicated that increased miR-187-3p suppresses Seipin expression in OGD/R PC12 cells. Therefore, experiments were performed to examine whether reduced Seipin expression is associated with impaired autophagic flux and increased apoptosis in OGD/R PC12 cells. Seipin expression was decreased in normoxic control (n=3; P<0.05) and OGD/R PC12 cells (n=3; P<0.05; Fig. 4A and B) following transfection of Seipin shRNA. In comparison with vehicle-treated PC12 cells, the levels of p62 (n=3; P<0.05; Fig. 4A and C) were elevated, the LC3II/I ratio was decreased (n=3; P<0.05; Fig. 4A and D), and the levels of cleaved caspase-3 (n=3; P<0.05; Fig. 4A and E) and Bax (n=3; P<0.05; Fig. 4A and F) were increased in normoxic control and OGD/R-treated PC12 cells following Seipin shRNA transfection. These results indicated that reduced Seipin expression disturbed autophagic flux and aggravated apoptosis in OGD/R PC12 cells.

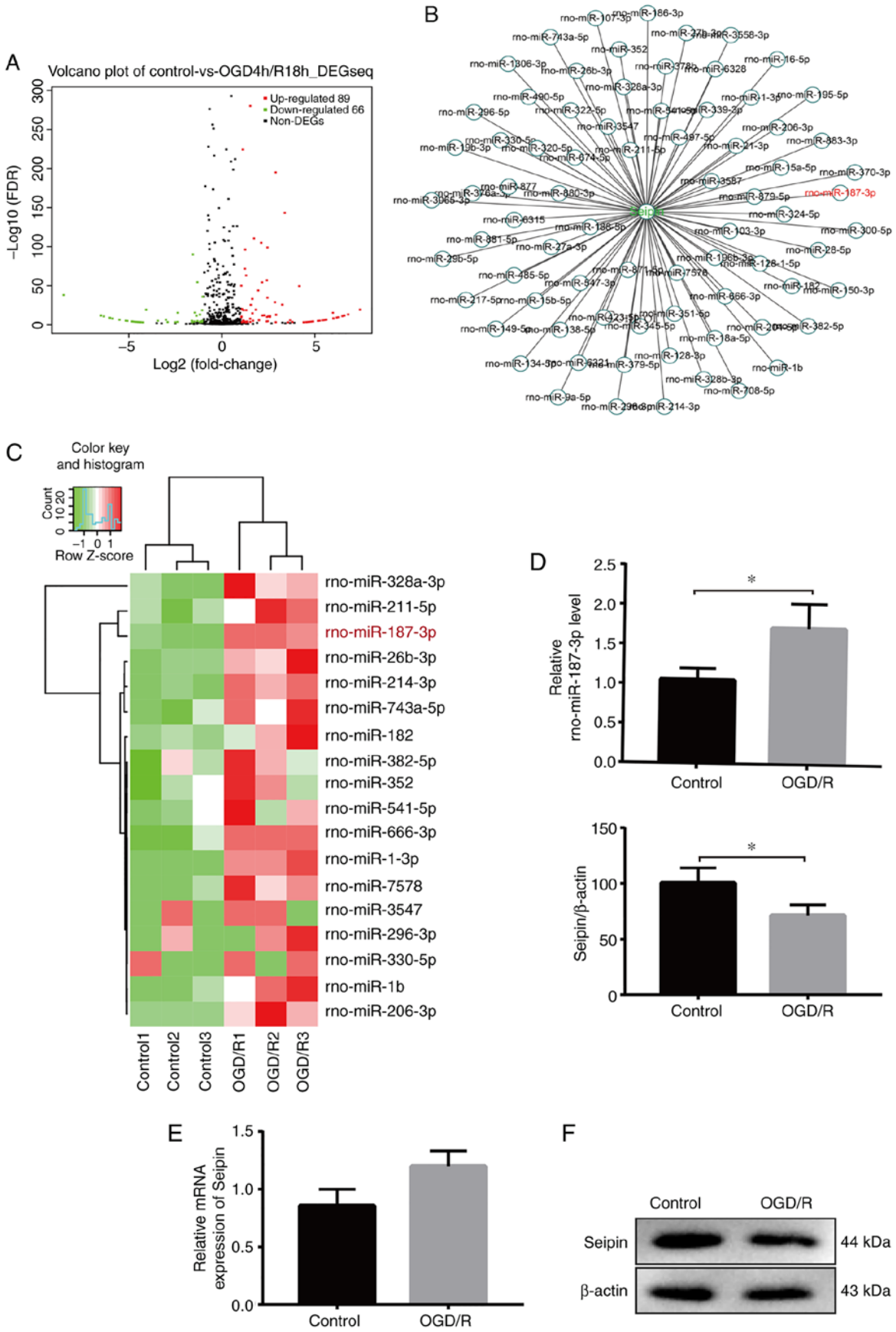

Figure 1. miR-187-3p is upregulated and Seipin protein is downregulated in PC12 cells after OGD/R. (A) After OGD/R, 89 miRNAs were upregulated and 66 were downregulated in PC12 cells. (B) Based on bioinformatics analysis, 76 miRNAs were predicted to target the coding sequence of Seipin. (C) Heatmap showing the significantly differential expression of 18 miRNAs after OGD/R, with fold-change >1. Highly expressed miRNAs are indicated in red, lowly expressed miRNAs in green. (D) miR-187-3p is upregulated in OGD/R PC12 cells. (E) Seipin mRNA expression is unchanged in OGD/R PC12 cells. (F) Western blot assay showing increased seipin protein in OGD/R compared with control cells. Data are the mean ± SD; n=3/group. *P<0.05. miR/miRNA, microRNA; OGD/R, oxygen-glucose deprivation and reoxygenation; rno, *Rattus norvegicus*; DEG, differentially expressed gene; FDR, false discovery rate.

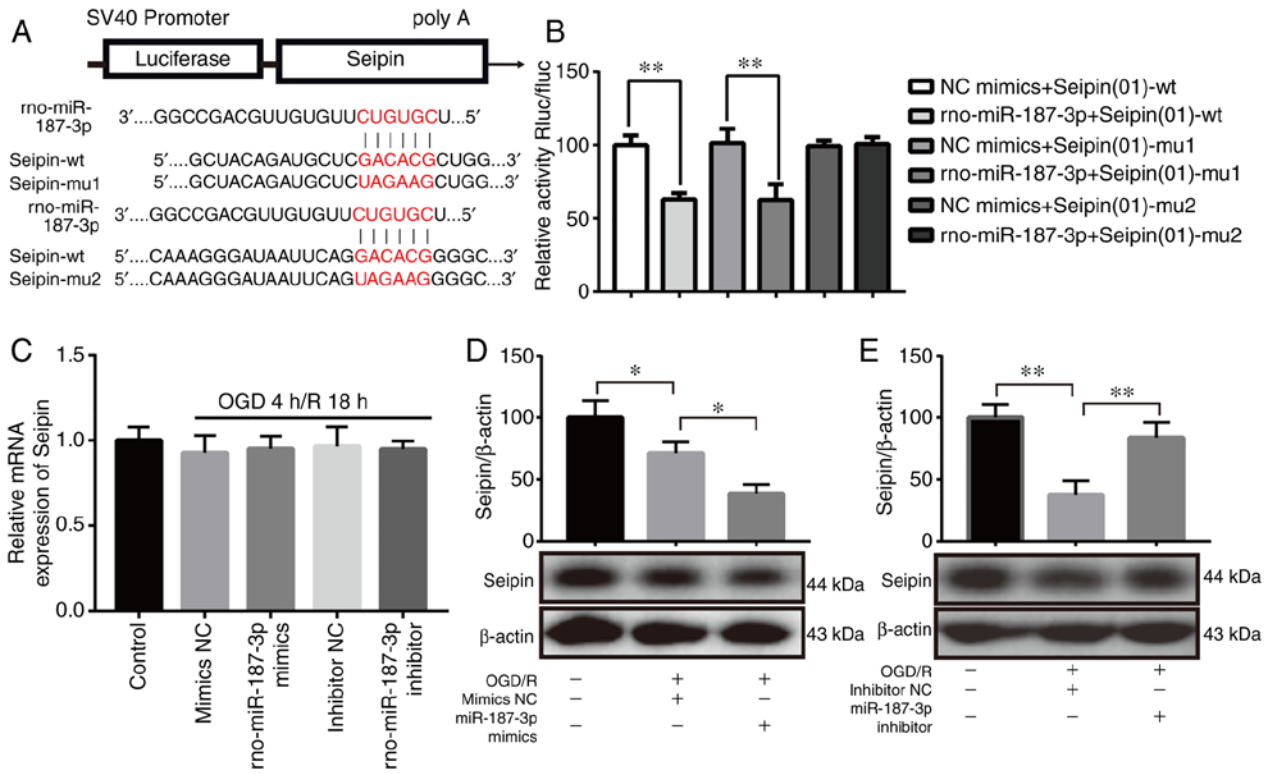

Figure 2. miR-187-3p regulates Seipin expression by directly targeting its CDS. (A) Schematic diagram showing the potential miR-187-3p binding sites in the seipin CDS. Two mutations were introduced in the Seipin CDS by replacing the wt binding sequence (GACACG) with a mutant sequence (UAGAAG). (B) Inhibition of the relative luciferase activity of the Seipin CDS reporter in 293T cells by miR-187-3p. (C) Seipin mRNA levels are unchanged after the addition of miR-187-3p mimics or inhibitor. (D) Western blot assay showing decreased Seipin protein in OGD/R + miR-187-3p mimic-treated cells when compared with OGD/R + mimic NC-treated cells. (E) Western blot assay showing increased Seipin protein in OGD/R + miR-187-3p inhibitor-treated cells when compared with OGD/R + inhibitor NC-treated cells. Data are the mean ± SD; n=3/group. *P<0.05, **P<0.01. miR, microRNA; OGD/R, oxygen-glucose deprivation and reoxygenation; NC, negative control; rno, *Rattus norvegicus*; CDS, coding sequence; wt, wild-type; mu, mutant; Rluc, *Renilla* luciferase; fluc, firefly luciferase.

Rapamycin does not rescue autophagy flux and apoptosis in Seipin knockdown PC12 cell after OGD/R. Seipin knockdown has been reported to reduce hippocampal autophagosome formation by enhancing Akt/mTOR activity (29). To investigate whether Seipin in PC12 cells regulated mTOR activity to regulate autophagic flux and apoptosis, the levels of phosphorylated (p-)mTOR were examined in PC12 cells. The levels of p-mTOR were lower in OGD/R-treated PC12 cells than normoxic controls; however, Seipin knockdown partially upregulated p-mTOR (n=3; P<0.05; Fig. 5A and B). Indeed, the administration of mTOR inhibitor rapamycin in Seipin shRNA-transfected PC12 cells failed to correct the increase in the level of p62 (n=3; P<0.05; Fig. 5A and C) and decrease in LC3II/I (n=3; P<0.05; Fig. 5A and D). Furthermore, rapamycin failed to correct the increase in cleaved caspase-3 (n=3; P<0.05; Fig. 5A and E) and Bax (n=3; P<0.05; Fig. 5A and F). The results indicated that reductions in Seipin expression disturbed autophagic flux and aggravated apoptosis in PC12 cells.

Seipin knockdown blocks miR-187-3p inhibitor-mediated neuroprotection in vitro. Next, it was examined whether Seipin knockdown would attenuate the effects on autophagic flux and apoptosis mediated by miR-187-3p inhibitor. The levels of p62 (n=3; P<0.05; Fig. 6A and B), cleaved caspase-3 (n=3; P<0.05; Fig. 6A and D) and Bax (n=3; P<0.05; Fig. 6A and E) were higher in OGD/R-treated PC12 cells than normoxic controls, whereas the LC3II/I ratio (n=3; P<0.05; Fig. 6A and C) was lower. Furthermore, flow cytometry revealed increased apoptosis in OGD/R-treated PC12 cells (Fig. 6F and G). Administration of miR-187-3p inhibitor in Seipin shRNA-transfected PC12 cells failed to rescue the increased levels of p62, apoptosis, cleaved caspase-3 and Bax, and the decreased LC3II/I ratio. The results suggested that the regulation of autophagic flux and apoptosis by miR-187-3p was dependent upon Seipin.

miR-187-3p antagomir reduces ischemia-induced infarction and upregulates Seipin-mediated autophagy in rats. A previous study reported that Seipin knockout in mice exacerbated cerebral damage induced by I/R (26). The *in vitro* results from the present study indicated that the OGD/R-induced increase in miR-187-3p expression and suppression of Seipin expression promoted neuronal apoptosis. Therefore, *in vitro* experiments examined the effect of miR-187-3p antagomir on ischemia-induced brain injury 24 h after 60 min of MCAO. The infarct volume was observed in MCAO rats, which was reduced by treatment with miR-187-3p antagomir (n=6; P<0.05; Fig. 7A and B). miR-187-3p antagomir was used to inhibit miR-187-3p expression in rats (n=6; P<0.05; Fig. 7C), which resulted in upregulation of Seipin (n=6; P<0.05; Fig. 7D) and LC3 (n=6; Fig. 7E).

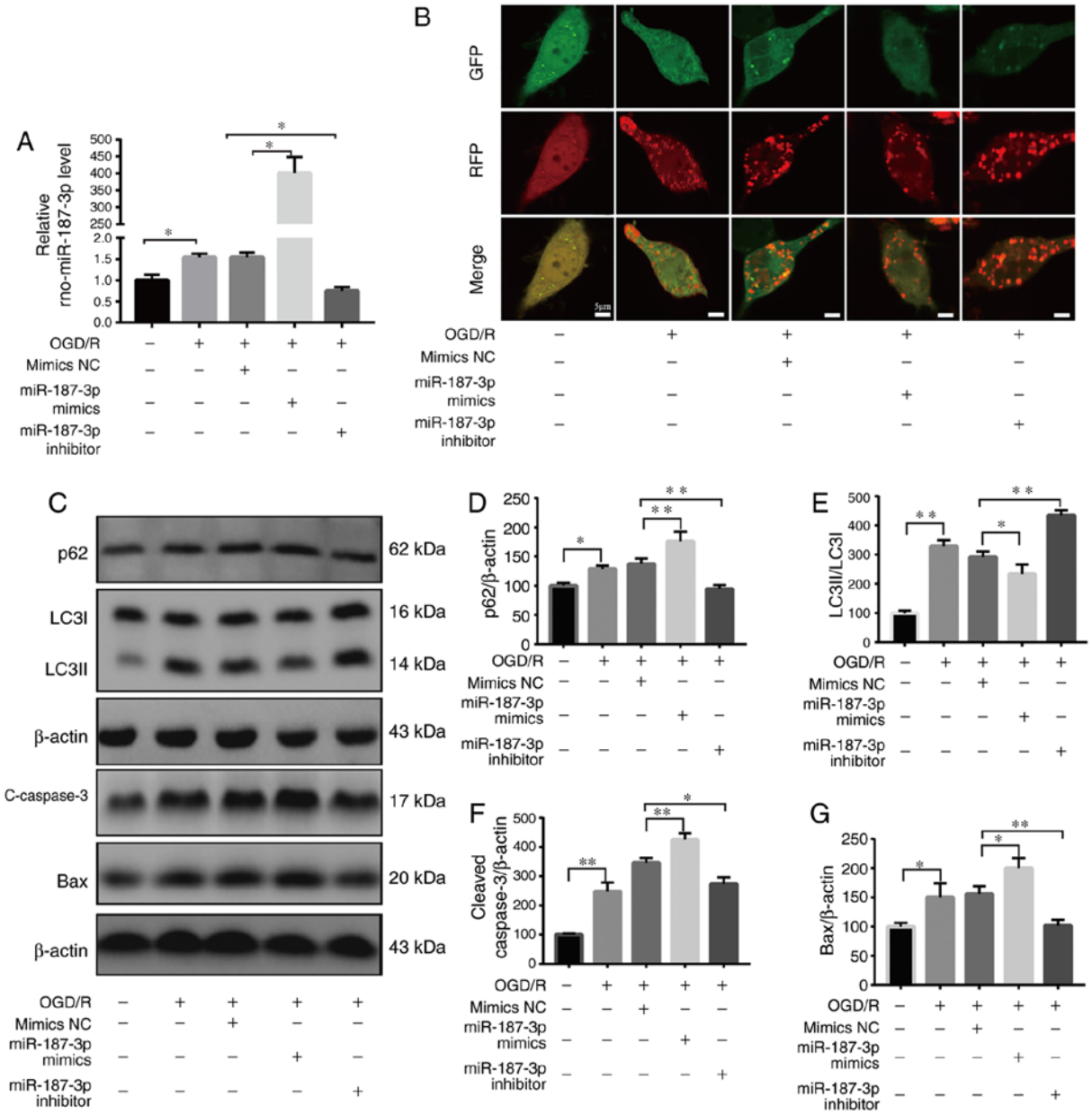

Figure 3. miR-187-3p regulates autophagic flux and apoptosis in OGD/R. (A) Transfection efficiency was determined by quantitative PCR. (B) Representative confocal images of GFP and RFP fluorescent puncta were observed by laser scanning confocal microscopy in PC12 cells treated with Ad-mRFP-GFP-LC3 plasmid. Scale bar=5 μm. (C) Representative western blots of autophagy- and apoptosis-related proteins in the different groups. Quantification (D) p62, (E) LC3II/LC3I, (F) c-caspase-3 and (G) Bax levels in OGD/R PC12 cells. Data are the mean ± SD; n=3/group. *P<0.05, **P<0.01. miR, microRNA; OGD/R, oxygen-glucose deprivation and reoxygenation; NC, negative control; rno, *Rattus norvegicus*; Ad, adenovirus; LC3, light chain 3; c-, cleaved.

Discussion

The present study present for the first time, to our knowledge, *in vivo* evidence that the ischemia-induced increase in miR-187-3p and subsequent suppression of Seipin expression led to deficits in autophagic flux and increased neuronal apoptosis. This conclusion is based on the following experimental data: i) OGD/R caused an increase in miR-187-3p expression and a decrease in Seipin protein levels; ii) bioinformatics analysis found miR-187-3p binding sites in the CDS of Seipin, and the reduction of Seipin protein in OGD/R-treated PC12 cells could be reversed by the inhibition of miR-187-3p; iii) autophagic flux was reduced in OGD/R-treated PC12 cells along with an increase in apoptosis-related protein expression, which was sensitive to the inhibition of miR-187-3p expression; iv) the impairment of autophagic flux and increase in neuronal apoptosis were aggravated in OGD/R-treated PC12 cells following Seipin knockdown, which was insensitive to inhibition of miR-187-3p; and v) the inhibition of miR-187-3p in a mouse model of cerebral I/R decreased the infarct volume.

In the present study, the level of Seipin mRNA was unchanged, but the level of Seipin protein was significantly decreased in OGD/R PC12 cells, which could be partially reversed by miR-187-3p inhibitor. The overexpression of miR-187-3p in PC12 cells reduced the level of Seipin protein. The results indicated that the increased miR-187-3p levels suppressed Seipin expression in OGD/R PC12 cells.

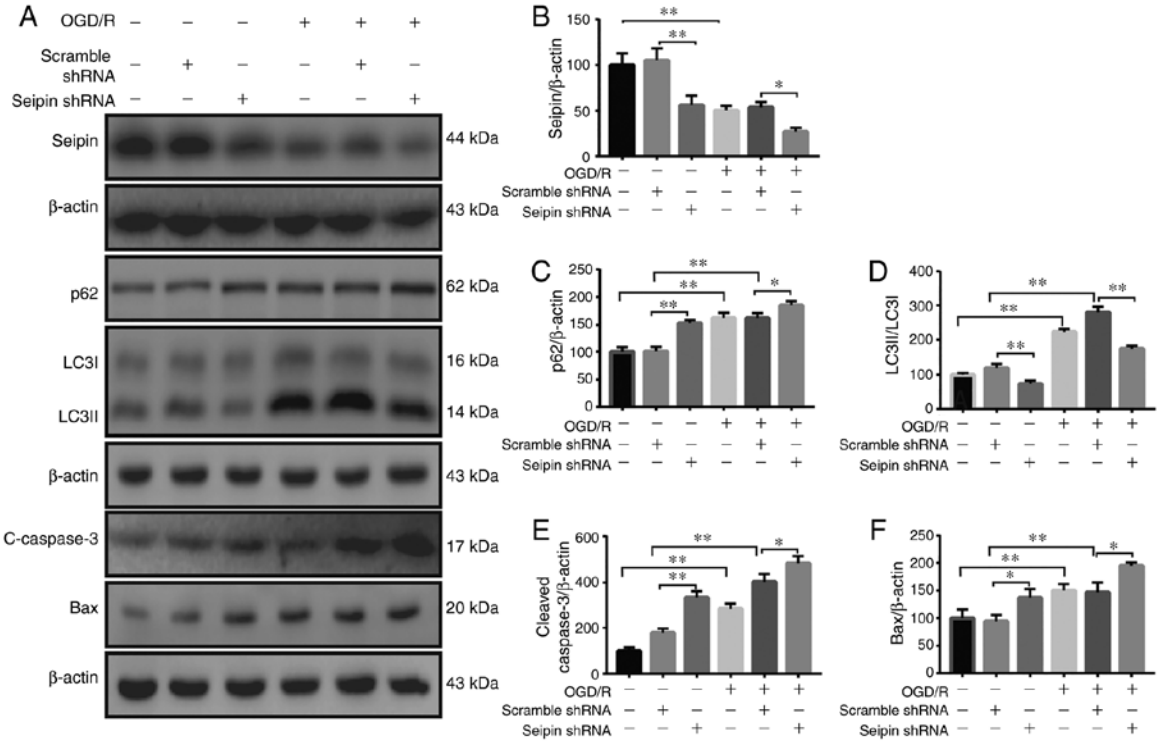

Figure 4. Seipin mediates autophagic flux and apoptosis in OGD/R PC12 cells. (A) Representative western blot images of Seipin, and autophagy- and apoptosis-related proteins in the different groups. (B) Quantitative analysis showing that Seipin protein levels are decreased significantly in PC12 cells after transfection with Seipin shRNA. Quantification of western blot data for (C) p62, (D) LC3II/LC3I, (E) c-caspase-3 and (F) Bax in normoxic control and OGD/R PC12 cells transfected with Seipin shRNA or scramble shRNA. Data are the mean ± SD; n=3/group. *P<0.05, **P<0.01. miR, microRNA; OGD/R, oxygen-glucose deprivation and reoxygenation; shRNA, short hairpin RNA; LC3, light chain 3; c-, cleaved.

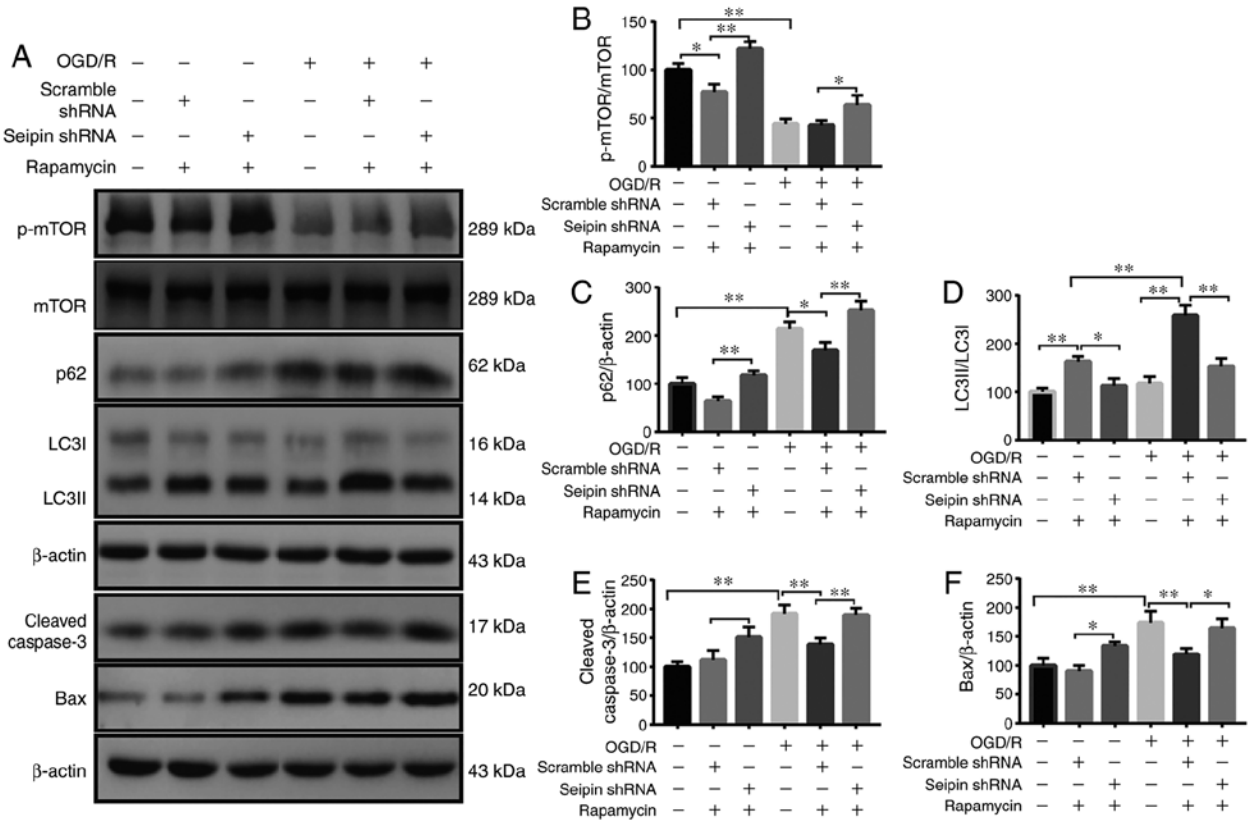

Figure 5. Effects of rapamycin on the expression of autophagy- and apoptosis-related proteins in Seipin-silenced PC12 cells. (A) Representative western blot images of the autophagy-related proteins p-mTOR, p62 and LC3II/I, and the apoptosis-related proteins c-caspase-3 and Bax in the different groups. Quantitative analysis of (B) p-mTOR/mTOR, (C) p62, (D) LC3II/LC3I, (E) c-caspase 3 and (F) Bax levels. Data are the mean ± SD; n=3/group. *P<0.05, **P<0.01. miR, microRNA; OGD/R, oxygen-glucose deprivation and reoxygenation; shRNA, short hairpin RNA; LC3, light chain 3; c-, cleaved; p-, phosphorylated.

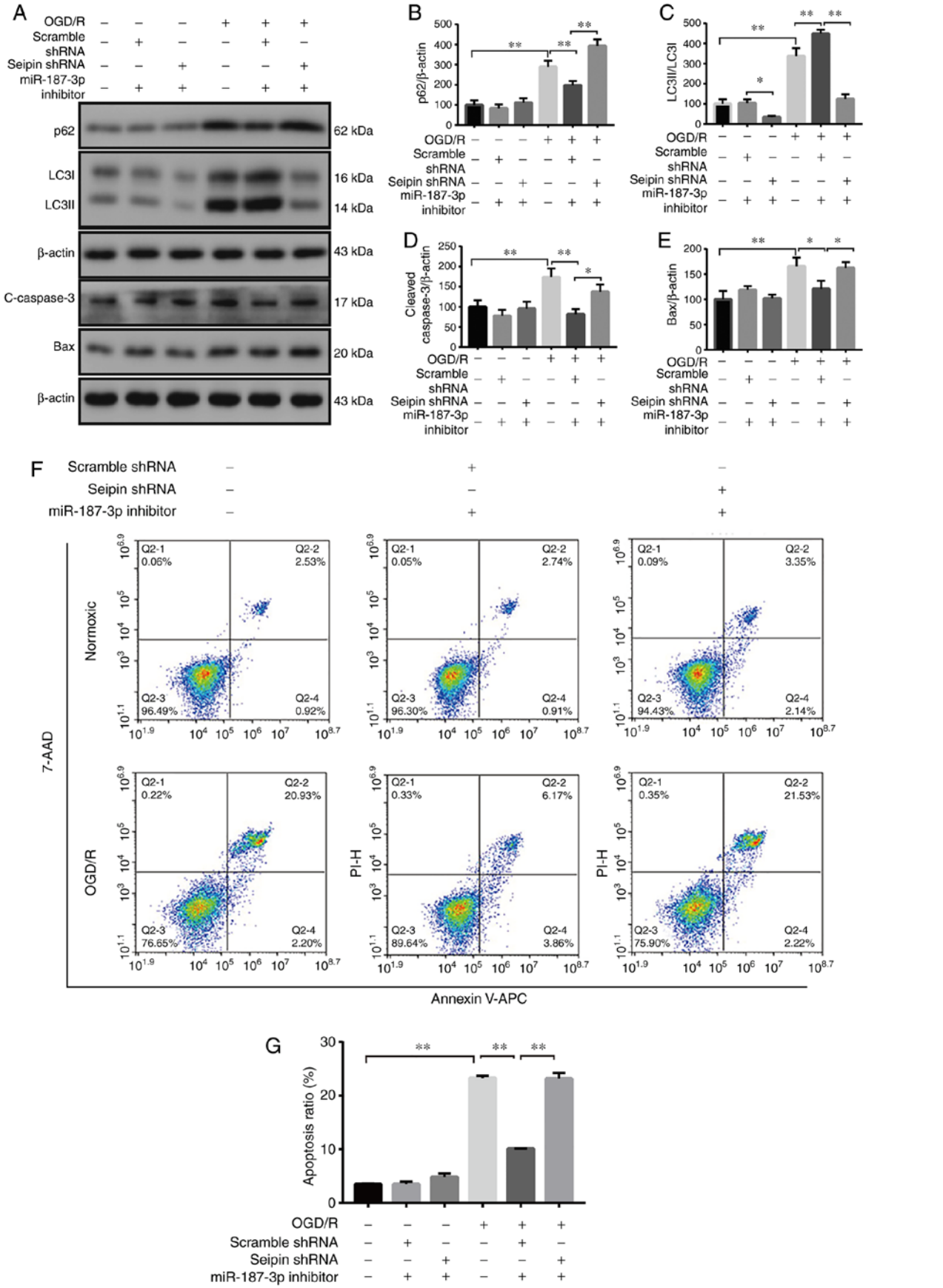

Figure 6. Effects of Seipin knockdown on autophagy and apoptosis mediated by miR-187-3p inhibitor in OGD/R PC12 cells. (A) Representative western blot images of the autophagy-related proteins p62 and LC3II/I, and the apoptosis-related proteins c-caspase-3 and Bax in the different groups. Quantitative analysis of (B) p62, (C) LC3II/LC3I, (D) c-caspase 3 and (E) Bax levels. (F) Flow cytometry assay and (G) quantification showing that Seipin knockdown abolishes miR-187-3p inhibitor-mediated neuroprotection in OGD/R-treated PC12 cells. Data are the mean ± SD; n=3/group. *P<0.05, **P<0.01. miR, microRNA; OGD/R, oxygen-glucose deprivation and reoxygenation; shRNA, short hairpin RNA; LC3, light chain 3; c-, cleaved; APC, allophycocyanin; 7-AAD, 7-aminoactinomyosin D.

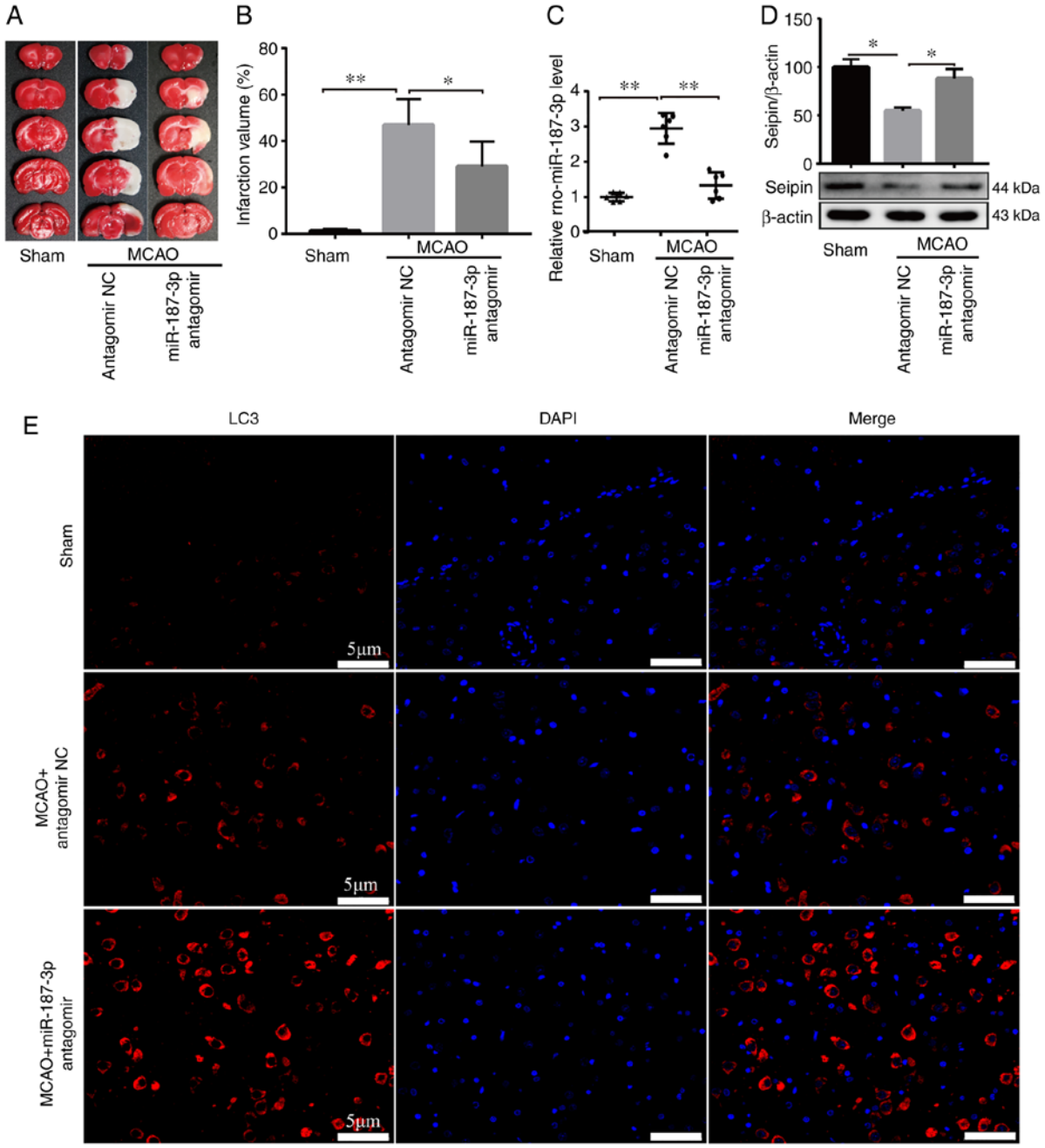

Figure 7. Administration of miR-187-3p antagomir reduces infarction via upregulating Seipin-mediated autophagy in a rat model of I/R. (A) Representative images of brain slices stained with tetrazolium chloride in antagomir NC and miR-187-3p antagomir-treated rats after I/R (1 h/24 h) or sham operation. (B) Quantitative analysis of the infarction volume in different groups. (C) miR-187-3p is downregulated in I/R rats by miR-187-3p antagomir. (D) Seipin protein expression is upregulated in I/R rats by miR-187-3p antagomir. (E) Double labeling immunofluorescence showed upregulation of LC3 by miR-187-3p antagomir. Scale bar=50 μm. Data are the mean ± SD; n=6/group. *P<0.05, **P<0.01. miR, microRNA; I/R, ischemia/reperfusion; MCAO, middle cerebral artery occlusion; NC, negative control; LC3, light chain 3; rno, *Rattus norvegicus*.

miR-187-3p has been identified as a cancer-related miRNA that plays promotive or suppressive roles in different malignancies (36-40). miR-187-3p inhibits the migration and invasion of hepatocellular carcinoma by suppressing S100 calcium-binding protein A4 (41). In mice, miR-187-3p mimic relieved I/R-induced pain hypersensitivity by inhibiting P2X7 receptor expression and subsequent mature IL-1β release (42).

Co-expression of human Seipin and ubiquitin showed that Seipin is polyubiquitinated, and its ubiquitination is enhanced by mutation (43); treatment of cells with a proteasome inhibitor increased the quantity of mutant Seipin in the cells, suggesting that it is degraded through the ER-associated degradation pathway. Of note, the N88S and S90L mutations are in the N-glycosylation motif, and these mutations enhance ubiquitination and degradation of Seipin via the ubiquitin-proteasome system (44). Conversely, the transcript encoding the long Seipin isoform (BSCL2-203, 462 aa) is expressed primarily in the brain, and its expression is inversely correlated with age in neuronal cells (24).

Autophagy plays a role in the pathophysiological process of ischemia-induced brain injury (45). The monitoring of autophagic flux is essential for estimating autophagic

activity. Autophagic flux is a dynamic process that involves the formation of autophagosomes, delivery of autophagic substrates to the autophagosomes and the degradation of these substrates (46). LC3I is post-translationally modified during autophagy induction to form LC3II; thus, LC3II/I is an index of autophagosome formation (47). LC3II/I, as an index of autophagosome formation, was increased in OGD/R-treated PC12 cells. The mammalian protein p62 is a selective autophagy substrate, continuously degraded by autophagy (48). It has been demonstrated that p62 binds directly to LC3, and this motif is required for autophagic degradation of p62 (49). Consistent with previous studies (50,51), the level of p62 was increased in OGD/R PC12 cells, indicating impaired autophagic flux. Of note, the decreased Seipin expression and impairment of autophagic flux in OGD/R PC12 cells could be ameliorated by the inhibition of miR-187-3p. In addition, knockdown of Seipin in OGD/R PC12 cells further aggravated the impairment of autophagic flux, which was insensitive to inhibition of miR-187-3p. The results supported the hypothesis that Seipin deficiency leads to an impairment in autophagic flux. mTOR signaling is a major negative regulator of autophagy (52). Neuronal Seipin deletion has been found to reduce autophagosome formation by enhancing mTOR signaling (29). The present findings indicated that a reduction in Seipin expression disturbed autophagic flux and aggravated apoptosis in in PC12 cells. Long-lasting autophagy or impaired autophagic flux induces type II programmed cell death (53-55). It was previously observed that the knockdown of Seipin exacerbated cerebral I/R-induced damage in mice (26). The increased expression of apoptosis-related proteins in OGD/R PC12 cells was corrected by the inhibition of miR-187-3p. Additionally, the knockdown of Seipin in OGD/R-treated PC12 cells further increased apoptosis, which was insensitive to the inhibition of miR-187-3p.

In conclusion, it was demonstrated that miR-187-3p inhibitor protected against OGD/R-induced apoptosis by upregulating Seipin-mediated autophagic flux in PC12 cells. It is hypothesized that enhanced activation of autophagic flux supports functional recovery, whereas impaired autophagic flux is associated with increased apoptosis. The present findings suggested that the miR-187-3p/Seipin axis has potential for the treatment of cerebral I/R injury in the future.

Acknowledgements

Not applicable.

Funding

This study was supported by grants from the National Natural Science Foundation of China (grant no. 81360199), Special Grant for Central Government Supporting Local Science and Technology Development, Science and Technology Department of Guizhou Province [grant no. (2019) 4008], Science and Technology Plan Project of Guizhou Province (Basic Science and Technology Cooperation) [grant no. (2020)1Z060], the Science and Technology Fund Project of Guizhou Health and Health Commission (grant no. gzwjkj2019-1-039), and the Science and Technology Fund Project of Southwest Guizhou Autonomous Prefecture (grant no. 2019-1-10).

Availability of data and materials

The datasets used and/or analyzed during the current study are available from the corresponding author on reasonable request.

Authors' contributions

WY and ZR designed the study. PX, JL and YH performed the experiments. ZR drafted the manuscript. ZG and LC contributed to the analysis of data and designed the animal experiment. All authors read and approved the final manuscript.

Ethics approval and consent to participate

The present study was approved by the Animal Care and Use Committee of Guizhou Medical University (approval no. 1900813).

Patient consent for publication

Not applicable.

Competing interests

The authors declare that they have no competing interests.

References

1. Lozano R, Naghavi M, Foreman K, Lim S, Shibuya K, Aboyans V, Abraham J, Adair T, Aggarwal R, Ahn SY, *et al*: Global and regional mortality from 235 causes of death for 20 age groups in 1990 and 2010: A systematic analysis for the Global Burden of Disease Study 2010. Lancet 380: 2095-2128, 2012.
2. Deng YH, He HY, Yang LQ and Zhang PY: Dynamic changes in neuronal autophagy and apoptosis in the ischemic penumbra following permanent ischemic stroke. Neural Regen Res 11: 1108-1114, 2016.
3. Cheon SY, Kim EJ, Kim SY, Kim JM, Kam EH, Park JK and Koo BN: Apoptosis signal-regulating kinase 1 silencing on astroglial inflammasomes in an experimental model of ischemic stroke. Neuroscience 390: 218-230, 2018.
4. Zhang S, An Q, Wang T, Gao S and Zhou G: Autophagy- and MMP-2/9-mediated reduction and redistribution of ZO-1 contribute to Hyperglycemia-increased blood-brain barrier permeability during early reperfusion in stroke. Neuroscience 377: 126-137, 2018.
5. Cassidy JM and Cramer SC: Spontaneous and therapeutic-induced mechanisms of functional recovery after stroke. Transl Stroke Res 8: 33-46, 2017.
6. Chan SJ, Love C, Spector M, Cool SM, Nurcombe V and Lo EH: Endogenous regeneration: Engineering growth factors for stroke. Neurochem Int 107: 57-65, 2017.
7. Spector WD, Limcangco R, Furukawa MF and Encinosa WE: The marginal costs of adverse drug events associated with exposures to anticoagulants and hypoglycemic agents during hospitalization. Med Care 55: 856-863, 2017.
8. Guo WT and Wang Y: Dgcr8 knockout approaches to understand microRNA functions in vitro and in vivo. Cell Mol Life Sci 76: 1697-1711, 2019.
9. Zhu H, Zhang Y, Tang R, Qu H, Duan X and Jiang Y: Banana sRNAome and degradome identify microRNAs functioning in differential responses to temperature stress. BMC Genomics 20: 33, 2019.
10. Blenkiron C, Askelund KJ, Shanbhag ST, Chakraborty M, Petrov MS, Delahunt B, Windsor JA and Phillips A: MicroRNAs in mesenteric lymph and plasma during acute pancreatitis. Ann Surg 260: 341-347, 2014.
11. Bartel DP: Metazoan MicroRNAs. Cell 173: 20-53, 2018.

12. El Fatimy R, Li S, Chen Z, Mushannen T, Gongala S, Wei Z, Balu DT, Rabinovsky R, Cantlon A, Elkhal A, *et al*: MicroRNA-132 provides neuroprotection for tauopathies via multiple signaling pathways. Acta Neuropathol 136: 537-555, 2018.
13. Huang W: MicroRNAs: Biomarkers, diagnostics, and therapeutics. Methods Mol Biol 1617: 57-67, 2017.
14. Han B, Zhang Y, Zhang Y, Bai Y, Chen X, Huang R, Wu F, Leng S, Chao J, Zhang JH, *et al*: Novel insight into circular RNA HECTD1 in astrocyte activation via autophagy by targeting MIR142-TIPARP: Implications for cerebral ischemic stroke. Autophagy 14: 1164-1184, 2018.
15. Du K, Zhao C, Wang L, Wang Y, Zhang KZ, Shen XY, Sun HX, Gao W and Lu X: MiR-191 inhibit angiogenesis after acute ischemic stroke targeting VEZF1. Aging (Albany NY) 11: 2762-2786, 2019.
16. Grimson A, Farh KK, Johnston WK, Garrett-Engele P, Lim LP and Bartel DP: MicroRNA targeting specificity in mammals: Determinants beyond seed pairing. Mol Cell 27: 91-105, 2007.
17. Duursma AM, Kedde M, Schrier M, le-Sage C and Agami R: MiR-148 targets human DNMT3b protein coding region. RNA 14: 872-877, 2008.
18. Tay Y, Zhang J, Thomson AM, Lim B and Rigoutsos I: MicroRNAs to Nanog, Oct4 and Sox2 coding regions modulate embryonic stem cell differentiation. Nature 455: 1124-1128, 2008.
19. Wang K, Li W, Bai Y, Yang W, Ling Y and Fang M: ssc-miR-7134-3p regulates fat accumulation in castrated male pigs by targetingMARK4gene. Int J Biol Sci 13: 189-197, 2017.
20. Ma L, Chen X, Li C, Cheng R, Gao Z, Meng X, Sun C, Liang C and Liu Y: miR-129-5p and -3p co-target WWP1 to suppress gastric cancer proliferation and migration. J Cell Biochem: Nov 11, 2018 (Epub ahead of print).
21. Su WC, Lin YH, Pagac M and Wang CW: Seipin negatively regulates sphingolipid production at the ER-LD contact site. J Cell Biol 218: 3663-3680, 2019.
22. Castro IG, Eisenberg-Bord M, Persiani E, Rochford JJ, Schuldiner M and Bohnert M: Promethin is a conserved seipin partner protein. Cells 8: 268, 2019.
23. Ding L, Yang X, Tian H, Liang J, Zhang F, Wang G, Wang Y, Ding M, Shui G and Huang X: Seipin regulates lipid homeostasis by ensuring calcium-dependent mitochondrial metabolism. EMBO J 37: e97572, 2018.
24. Sánchez-Iglesias S, Fernández-Liste A, Guillín-Amarelle C, Rábano A, Rodriguez-Cañete L, González-Méndez B, Fernández-Pombo A, Senra A and Araújo-Vilar D: Does seipin play a role in oxidative stress protection and peroxisome biogenesis? New insights from human brain autopsies. Neuroscience 396: 119-137, 2019.
25. Ito D, Fujisawa T, Iida H and Suzuki N: Characterization of seipin/BSCL2, a protein associated with spastic paraplegia 17. Neurobiol Dis 31: 266-277, 2008.
26. Chen Y, Wei L, Tian J, Wang YH, Liu G and Wang C: Seinpin knockout exacerbates cerebral ischemia/reperfusion damage in mice. Biochem Biophys Res Commun 474: 377-383, 2016.
27. Zowalaty AEE and Ye X: Seipin deficiency leads to defective parturition in mice. Biol Reprod 97: 378-386, 2017.
28. Fan HD, Chen SP, Sun YX, Xu SH and Wu LJ: Seipin mutation at glycosylation sites activates autophagy in transfected cells via abnormal large lipid droplets generation. Acta Pharmacol Sin 36: 497-506, 2015.
29. Chang H, Di T, Wang Y, Zeng X, Li G, Wan Q, Yu W and Chen L: Seipin deletion in mice enhances phosphorylation and aggregation of tau protein through reduced neuronal PPARγ and insulin resistance. Neurobiol Dis 127: 350-361, 2019.
30. Tao J, Liu W, Shang G, Zheng Y, Huang J, Lin R and Chen L: miR-207/352 regulate lysosomal-associated membrane proteins and enzymes following ischemic stroke. Neuroscience 305: 1-14, 2015.
31. Chen F, Zhang L, Wang E, Zhang C and Li X: LncRNA GAS5 regulates ischemic stroke as a competing endogenous RNA for miR-137 to regulate the Notch1 signaling pathway. Biochem Biophys Res Commun 496: 184-190, 2018.
32. Livak KJ and Schmittgen TD: Analysis of relative gene expression data using real-time quantitative PCR and the 2(-Delta Delta C(T)) method. Methods 25: 402-408, 2001.
33. Yan H, Yuan J, Gao L, Rao J and Hu J: Long noncoding RNA MEG3 activation of p53 mediates ischemic neuronal death in stroke. Neuroscience 337: 191-199, 2016.
34. Slott VL, Linder RE and Dyer CJ: Method of euthanasia does not affect sperm motility in the laboratory rat. Reprod Toxicol 8: 371-374, 1994.
35. Hu Q, Manaenko A, Bian H, Guo Z, Huang JL, Guo ZN, Yang P, Tang J and Zhang JH: Hyperbaric oxygen reduces infarction volume and hemorrhagic transformation through ATP/NAD^+/Sirt1 pathway in hyperglycemic middle cerebral artery occlusion rats. Stroke 48: 1655-1664, 2017.
36. Sun C, Li S, Yang C, Xi Y, Wang L, Zhang F and Li D: MicroRNA-187-3p mitigates non-small cell lung cancer (NSCLC) development through down-regulation of BCL6. Biochem Biophys Res Commun 471: 82-88, 2016.
37. Zhao J, Lei T, Xu C, Li H, Ma W, Yang Y, Fan S and Liu Y: MicroRNA-187, down-regulated in clear cell renal cell carcinoma and associated with lower survival, inhibits cell growth and migration though targeting B7-H3. Biochem Biophys Res Commun 438: 439-444, 2013.
38. Casanova-Salas I, Masiá E, Armiñán A, Calatrava A, Mancarella C, Rubio-Briones J, Scotlandi K, Vicent MJ and López-Guerrero JA: MiR-187 targets the androgen-regulated gene ALDH1A3 in prostate cancer. PLoS One 10: e0125576, 2015.
39. Zhang F, Luo Y, Shao Z, Xu L, Liu X, Niu Y, Shi J, Sun X, Liu Y, Ding Y and Zhao L: MicroRNA-187, a downstream effector of TGFβ pathway, suppresses Smad-mediated epithelial-mesenchymal transition in colorectal cancer. Cancer Lett 373: 203-213, 2016.
40. Mulrane L, Madden SF, Brennan DJ, Gremel G, McGee SF, McNally S, Martin F, Crown JP, Jirström K, Higgins DG, *et al*: miR-187 is an independent prognostic factor in breast cancer and confers increased invasive potential in vitro. Clin Cancer Res 18: 6702-6713, 2012.
41. Dou C, Liu Z, Xu M, Jia Y, Wang Y, Li Q, Yang W, Zheng X, Tu K and Liu Q: MiR-187-3p inhibits the metastasis and epithelial-mesenchymal transition of hepatocellular carcinoma by targeting S100A4. Cancer Lett 381: 380-390, 2016.
42. Li XQ, Yu Q, Zhang ZL, Sun XJ and Ma H: MiR-187-3p mimic alleviates ischemia-reperfusion-induced pain hypersensitivity through inhibiting spinal P2X7R and subsequent mature IL-1β release in mice. Brain Behav Immun 79: 91-101, 2019.
43. Ito D and Suzuki N: Seipin/BSCL2-related motor neuron disease: Seipinopathy is a novel conformational disease associated with endoplasmic reticulum stress. Rinsho Shinkeigaku 47: 329-335, 2007 (In Japanese).
44. Ito D, Yagi T, Ikawa M and Suzuki N: Characterization of inclusion bodies with cytoprotective properties formed by seipinopathy-linked mutant seipin. Hum Mol Genet 21: 635-646, 2012.
45. Wang P, Xu TY, Wei K, Guan YF, Wang X, Xu H, Su DF, Pei G and Miao CY: ARRB1/β-arrestin-1 mediates neuroprotection through coordination of BECN1-dependent autophagy in cerebral ischemia. Autophagy 10: 1535-1548, 2014.
46. Iwai-Kanai E, Yuan H, Huang C, Sayen MR, Perry-Garza CN, Kim L and Gottlieb RA: A method to measure cardiac autophagic flux in vivo. Autophagy 4: 322-329, 2008.
47. Holt SV, Wyspianska B, Randall KJ, James D, Foster JR and Wilkinson RW: The development of an immunohistochemical method to detect the autophagy-associated protein LC3-II in human tumor xenografts. Toxicol Pathol 39: 516-523, 2011.
48. Pankiv S, Clausen TH, Lamark T, Brech A, Bruun JA, Outzen H, Øvervatn A, Bjørkøy G and Johansen T: p62/SQSTM1 binds directly to Atg8/LC3 to facilitate degradation of ubiquitinated protein aggregates by autophagy. J Biol Chem 282: 24131-24145, 2007.
49. Johansen T and Lamark T: Selective autophagy mediated by autophagic adapter proteins. Autophagy 7: 279-296, 2011.
50. Liu X, Tian F, Wang S, Wang F and Xiong L: Astrocyte autophagy flux protects neurons against oxygen-glucose deprivation and ischemic/reperfusion injury. Rejuvenation Res 21: 405-415, 2018.
51. Jiang H, Ma Y, Yan J, Liu J and Li L: Geniposide promotes autophagy to inhibit insulin resistance in HepG2 cells via P62/NF-κB/GLUT-4. Mol Med Rep 16: 7237-7244, 2017.
52. Zhao Z, Han F, Yang S, Wu J and Zhan W: Oxamate-mediated inhibition of lactate dehydrogenase induces protective autophagy in gastric cancer cells: Involvement of the Akt-mTOR signaling pathway. Cancer Lett 358: 17-26, 2015.
53. Adhami F, Liao G, Morozov YM, Schloemer A, Schmithorst VJ, Lorenz JN, Dunn RS, Vorhees CV, Wills-Karp M, Degen JL, *et al*: Cerebral ischemia-hypoxia induces intravascular coagulation and autophagy. Am J Pathol 169: 566-583, 2006.
54. Ouyang L, Shi Z, Zhao S, Wang FT, Zhou TT, Liu B and Bao JK: Programmed cell death pathways in cancer: A review of apoptosis, autophagy and programmed necrosis. Cell Prolif 90: 487-498, 2012.
55. McCrary MR, Jiang MQ, Giddens MM, Zhang JY, Owino S, Wei ZZ, Zhong W, Gu X, Xin H, Hall RA, *et al*: Protective effects of GPR37 via regulation of inflammation and multiple cell death pathways after ischemic stroke in mice. FASEB J 33: 10680-10691, 2019.